Vapor−Liquid Equilibria of Binary and Ternary Mixtures Containing Methane, Ethane, and Carbon Dioxide from Gibbs Ensemble Simulations

Anping Liu and Thomas L. Beck*

Department of Chemistry, University of Cincinnati, Cincinnati, Ohio 45221-0172

Received: November 5, 1997; In Final Form: March 17, 1998

Simulations are presented of the liquid-phase−vapor-phase equilibria of binary mixtures (methane + ethane, methane + carbon dioxide, ethane + carbon dioxide) and ternary mixtures (methane + ethane + carbon dioxide) in the Gibbs ensemble. Methane, ethane, and carbon dioxide are described with molecular models of the types 1CLJ, 2CLJ, and 2CLJQ, respectively. The equality of the chemical potentials in the two phases is maintained by transfer of the smallest molecule and exchange for the remaining molecules. The successful acceptance ratio of exchange is usually more than 10 times larger than that for transfer. The results are in relatively good agreement with experimental and other simulation data.

1. Introduction

Since the Gibbs ensemble simulation technique was developed by Panagiotopoulos[1] in 1987, it has been widely applied to the study of phase behavior of pure fluids and mixtures due to its simplicity and directness.[2] So far, most of the applications of the method for mixtures have involved spherical Lennard-Jones particles;[3−5] extensive phase information has been computed for relatively long chain single component alkane species,[6,7] but to our knowledge the recent study by Martin and Siepmann[8] of alkane mixture phase equilibria is the only example to date of simulations performed in the Gibbs ensemble for real mixtures (binary or ternary) with accurate intermolecular potentials. Recently, Vrabec and Fischer applied the *NpT* + test particle method to ternary mixtures containing methane, ethane, and carbon dioxide,[9] which are described as one- or two-center Lennard-Jones fluids. Their results showed that the potentials they used are quite accurate for the binary mixtures as well as for the ternary mixtures. Here we apply the Gibbs ensemble method to the same system with the same potentials in order to compare the results obtained with the two widely different approaches and with experimental data. Both methods yield good agreement with experiment, and these independent results imply that the methods are effective and the intermolecular potentials are relatively accurate.

The key step in the Gibbs ensemble is the particle transfer. For linear molecules, the transfer of particles between the two simulation boxes becomes considerably more difficult than for spherical particles. Recently, it has been shown that the chemical potential difference between linear particles can be accurately determined by the energy difference method,[10] in which particles are fictively switched into the other component during the course of the simulation and the distribution of energy differences yields the chemical potential difference. Therefore, it is appropriate to utilize in our simulations the procedure proposed by Panagiotopoulos[11] which is designed for mixtures containing components very different in size and shape. In that procedure, the chemical potential equality of the components in the system is obtained through the transfer of particles of the smaller component and the exchange of particles for the remaining components. In the present study, methane, ethane, and carbon dioxide are described by effective potentials using molecular models of 1CLJ (one-center-Lennard-Jones), 2CLJ (two-centers-Lennard-Jones), and 2CLJQ (two-centers-Lennard-Jones plus point quadrupole), respectively.[9,12,13] Thus, the exchange of particles for 1C−2C and 2C−2C is involved in the simulations of these mixtures. Here we report simulation results for binary and ternary mixtures of methane, ethane, and carbon dioxide at $T = 250$ K and over a pressure range of $P =$ 14−80 bar.

2. The Method

The methodology of the Gibbs ensemble has been described in detail elsewhere.[1,11] Here we list the formulas used in our simulations for the convenience of the reader.

Each trial move is accepted with a probability as follows:

(a) particle displacements

$$P_{\text{move}} = \min[1, \exp(-\beta\Delta E)] \tag{1}$$

where ΔE is the energy change for the trial move in box I or II;

(b) volume rearrangement in the constant *NpT* ensemble[3]

$$P_{\text{vol}} = \min\left[1, \exp\left(-\beta\left(\Delta E^{\text{I}} + \Delta E^{\text{II}} - N^{\text{I}}kT\ln\left(\frac{V^{\text{I}} + \Delta V^{\text{I}}}{V^{\text{I}}}\right) - N^{\text{II}}kT\ln\left(\frac{V^{\text{II}} + \Delta V^{\text{II}}}{V^{\text{II}}}\right) + P(\Delta V^{\text{I}} + \Delta V^{\text{I}})\right)\right)\right] \tag{2}$$

where ΔV^{I} and $-\Delta V^{\text{II}}$ are independent volume changes in box I and box II, respectively;

(c) particle transfer

$$P_{\text{trans}} = \min\left[1, \exp\left(-\beta\left(\Delta E^{\text{I}} + \Delta E^{\text{II}} + kT\ln\left(\frac{V^{\text{II}}(N_i^{\text{I}} + 1)}{V^{\text{I}}N_i^{\text{II}}}\right)\right)\right)\right] \tag{3}$$

where a particle of component *i* is inserted into box I and a particle of the same component is removed from box II;

S1089-5647(98)00094-7 CCC: $15.00
Published on Web 09/01/1998

(d) particle exchange

$$P_{\text{exch}} = \min\left[1, \exp\left(-\beta\left(\Delta E^{\text{I}} + \Delta E^{\text{II}} + kT\ln\left(\frac{V^{\text{II}}(N_i^{\text{I}}+1)}{V^{\text{I}}N_i^{\text{II}}}\right) + kT\ln\left(\frac{V^{\text{I}}(N_j^{\text{II}}+1)}{V^{\text{II}}N_j^{\text{I}}}\right)\right)\right)\right] \quad (4)$$

where a particle of component j is switched to a particle of component i in box I and a particle of component i is switched to a particle of component j in box II at the same time. Theoretically, the procedure for particle exchange can be applied to any component in the system, but it is apparent that the transfer should be applied to the smaller particle and the exchange to the larger particles. The equilibrium conditions of the two phases are satisfied with steps a−d:

$$T^{\text{I}} = T^{\text{II}}$$
$$P^{\text{I}} = P^{\text{II}}$$
$$\mu_i^{\text{I}} = \mu_i^{\text{II}}$$
$$\Delta\mu_{ji}^{\text{I}} = \Delta\mu_{ji}^{\text{II}} \quad (5)$$

The residual chemical potentials and the residual chemical potential differences can be calculated during the simulation:[14]

$$\mu_{i,\text{res}}^{\text{I}} = -kT\ln\left\langle\frac{V^{\text{I}}}{N_i^{\text{I}}+1}\exp(-\beta\Delta E_i^{\text{I}})\right\rangle \quad (6)$$

$$\Delta\mu_{ji,\text{res}}^{\text{I}} = -kT\ln\left\langle\frac{N_i^{\text{I}}}{N_j^{\text{I}}}\exp(-\beta\Delta E_{ji}^{\text{I}})\right\rangle \quad (7)$$

where ΔE_i^{I} is the energy of the particle to be inserted in box I and ΔE_{ji}^{I} is the energy difference between the components j and i. $\langle ... \rangle$ denotes the Gibbs ensemble average. The formulas above can also apply to calculations in box II.

3. Molecular Models

In our simulations we used the effective pair potentials determined by Lotfi et al.[12,13] for CH_4-CH_4, $C_2H_6-C_2H_6$, CO_2-CO_2, $CH_4-C_2H_6$, CH_4-CO_2, and $CO_2-C_2H_6$, which were obtained by fitting experimental data using the NpT + test particle method. All interactions were of the Lennard-Jones type except for the point quadrupole interaction between CO_2 molecules. The parameters for the three like interactions are presented in Table 1, and the unlike interaction parameters are presented in Table 2.

The unlike interactions ij are expressed through the unlike interaction parameters η and ξ and the like potential parameters as

$$\sigma_{ij} = {}^1/_2\eta(\sigma_i + \sigma_j) \quad (8)$$

$$\epsilon_{ij} = \xi[\epsilon_i\epsilon_j]^{1/2} \quad (9)$$

In the simulations of the ternary system, no ternary parameters were introduced; the six different pairwise interactions from the binary systems were used to model the interactions.

4. Simulation Details

Constant pressure Gibbs ensemble Monte Carlo simulations were carried out for binary and ternary mixtures containing methane, ethane, and carbon dioxide, which are different in size and energy parameters as well as molecular models. The phase equilibrium was achieved through displacement of particles within each box, volume changes, and particle transfer/exchange between the two boxes. A total of 512 particles was used in each simulation with a cutoff radius of $3.5\sigma_A$. The starting configurations were fcc at densities and concentrations taken from literature data. The first 1500 cycles were for equilibration with 1500−2500 cycles for the production runs. A cycle contained displacement of each particle in turn within each box and 200−400 trial transfers/exchanges which ensured at least 5000 successful transfers/exchanges of each component during the run. The acceptance rates for some mixtures are presented in Table 3. Since the acceptance rates of exchanges were as high as 10 times that of transfers, portions of the total trials were assigned to transfer and exchange moves so that each component had about the same number of successful moves. Pressures and chemical potentials were calculated to monitor the process. Uncertainties were estimated from block averages.

Methane is modeled as a one-center Lennard-Jones particle, ethane as a two-center Lennard-Jones particle, and carbon dioxide as a two-center Lennard-Jones particle plus point quadrupole. Exchanging methane with ethane has two steps: a symmetric stretch of the two sites around the center and random orientation. Exchanging ethane to methane corresponds to simply shrinking the two sites to the center with the parameters of methane. The same procedure was applied for the exchange of methane and carbon dioxide. For the exchange of ethane and carbon dioxide, the orientations were kept and the sites were obtained by shrinking or stretching according to the fixed bond lengths. In the binary mixtures $CH_4-C_2H_6$ and CH_4-CO_2, particle transfers were applied to CH_4 and exchanges were applied to CH_4/C_2H_6 and CH_4/CO_2. In the binary mixture $CO_2-C_2H_6$, transfer was applied to CO_2 and exchange to CO_2-

TABLE 1: Parameters for Molecular Interactions for Methane, Ethane, and Carbon Dioxide Modeled as 1CLJ, 2CLJ, and 2CLJQ Fluids, Respectively ($L^* = l/\sigma$; $(Q^*)^2 = Q^2/(\epsilon\sigma^5)$)

substance	σ, Å	ϵ/k, K	L^*	$(Q^*)^2$
methane	3.7275	148.99		
ethane	3.5000	135.57	0.67	
carbon dioxide	3.0354	125.317	0.699	3.0255

TABLE 2: Unlike Interaction Parameters for the Three Binary Mixtures

mixture	η	ξ
methane + ethane	1.001 40	0.999 23
methane + carbon dioxide	0.992 20	0.955 80
ethane + carbon dioxide	1.000 00	0.946 91

TABLE 3: Acceptance Rates (Given as Percentages) for the Binary and Ternary Mixtures at Different Pressures along the Coexistence Curves

system	P, bar	r_A	r_{AB}	r_{AC}
$CH_4-C_2H_6$	15.1	2.0	19.4	
	40.0	4.6	22.9	
	60.0	8.5	26.5	
CH_4-CO_2	40.0	1.1	17.1	
	60.0	2.0	19.9	
	80.0	9.4	36.4	
$CO_2-C_2H_6$	15.0	1.6	35.9	
	18.0	1.8	33.3	
	20.0	1.3	28.8	
	18.0	0.4	19.8	
CH_4-CO_2-C_2H_6	30.4	3.2	34.7	20.7
		2.9	27.5	18.8
		1.8	19.8	15.1

TABLE 4: Simulation Results for the Binary Mixture $CH_4 + C_2H_6$ at $T = 250$ K[a]

P^*	P^{*I}	P^{*II}	x_A^I	x_A^{II}	ρ^{*I}	ρ^{*II}	$\beta\mu_A^{*I}$	$\beta\mu_A^{*II}$	$\beta\Delta\mu_{BA}^{*I}$	$\beta\Delta\mu_{BA}^{*II}$	$\beta\Delta\mu_{AB}^{*I}$	$\beta\Delta\mu_{AB}^{*II}$
0.038	0.046 (8)	0.038 (1)	0.020 (1)	0.125 (1)	0.4671 (22)	0.0280 (1)	−5.56 (4)	−5.83 (2)	1.62 (5)	1.75 (1)	−1.54 (4)	−1.68 (1)
0.050	0.050 (6)	0.050 (1)	0.088 (4)	0.374 (6)	0.4590 (13)	0.0367 (1)	−4.46 (2)	−4.50 (1)	0.25 (6)	0.31 (2)	−0.91 (38)	−0.28 (4)
0.076	0.063 (20)	0.075 (1)	0.177 (2)	0.528 (2)	0.4517 (27)	0.0573 (7)	−3.77 (3)	−3.80 (2)	−0.48 (4)	−0.44 (3)	1.25 (1)	0.47 (3)
0.101	0.092 (90)	0.101 (1)	0.293 (6)	0.641 (4)	0.4457 (60)	0.0822 (1)	−3.31 (1)	−3.34 (1)	−0.98 (3)	−1.00 (5)	1.07 (30)	1.05 (1)
0.126	0.118 (4)	0.122 (1)	0.367 (3)	0.682 (3)	0.4383 (58)	0.1080 (10)	−3.10 (1)	−3.10 (1)	−1.22 (2)	−1.26 (2)	1.84 (17)	1.32 (2)
0.151	0.140 (15)	0.149 (2)	0.473 (9)	0.688 (3)	0.3977 (93)	0.1597 (79)	−2.94 (4)	−2.90 (3)	−1.49 (5)	−1.49 (5)	1.99 (6)	1.38 (10)
0.164	0.173 (9)	0.164 (3)	.0.514 (6)	0.67 (9)4	0.4079 (87)	0.2311 (57)	−2.79 (1)	−2.76 (2)	−1.67 (5)	−1.70 (1)	2.18 (3)	−1.75 (4)

[a] The numbers in parentheses indicate the statistical uncertainties in the last digits. $P^* = p\sigma^3/\epsilon$; $\rho^* = \rho\sigma^3$; $\mu^* = \mu/\epsilon$.

TABLE 5: Simulation Results for the Binary Mixture $CH_4 + CO_2$ at $T = 250$ K[a]

P^*	P^{*I}	P^{*II}	x_A^I	x_A^{II}	ρ^{*I}	ρ^{*II}	$\beta\mu_A^{*I}$	$\beta\mu_A^{*II}$	$\beta\Delta\mu_{BA}^{*I}$	$\beta\Delta\mu_{BA}^{*II}$	$\beta\Delta\mu_{AB}^{*I}$	$\beta\Delta\mu_{AB}^{*II}$
0.076	0.054 (7)	0.076 (1)	0.040 (2)	0.326 (1)	0.7195 (29)	0.0572 (4)	−4.15 (1)	−4.24 (1)	0.65 (10)	0.52 (1)	−0.11 (1)	−0.48 (2)
0.101	0.115 (21)	0.099 (4)	0.082 (4)	0.479 (8)	0.7119 (55)	0.0747 (7)	−3.65 (8)	−3.65 (3)	0.10 (10)	−0.18 (6)	0.58 (1)	0.14 (3)
0.126	0.156 (36)	0.125 (4)	0.131 (2)	0.558 (3)	0.6834 (27)	0.1012 (26)	−3.26 (2)	−3.25 (2)	−0.36 (6)	−0.53 (1)	0.83 (3)	0.50 (1)
0.151	0.126 (28)	0.154 (2)	0.197 (5)	0.612 (1)	0.6614 (31)	0.1340 (17)	−3.02 (5)	−3.03 (1)	−0.56 (2)	−0.84 (1)	1.10 (2)	0.79 (1)
0.176	0.172 (6)	0.175 (5)	0.304 (25)	0.646 (2)	0.5759 (22)	0.1516 (1)	−2.92 (1)	−2.90 (2)	−0.90 (14)	−0.89 (4)	1.13 (1)	0.85 (2)
0.194	0.192 (7)	0.195 (1)	0.397 (15)	0.647 (5)	0.5153 (165)	0.1899 (8)	−2.79 (16)	−2.78 (16)	−1.17 (30)	−1.13 (8)	1.21 (1)	1.09 (3)
0.201	0.192 (11)	0.199 (2)	0.429 (15)	0.655 (13)	0.4623 (320)	0.1961 (14)	−2.80 (3)	−2.77 (3)	−1.01 (3)	−1.26 (11)	1.09 (6)	0.89 (7)

[a] The numbers in parentheses indicate the statistical uncertainties in the last digits. $P^* = \rho\sigma^3/\epsilon$; $\rho^* = \rho\sigma^3$; $\mu^* = \mu/\epsilon$.

TABLE 6: Simulation Results for the Binary Mixture $CO_2 + C_2H_6$ at $T = 250$ K[a]

P^*	P^{*I}	P^{*II}	x_A^{II}	x_A^{II}	ρ^{*I}	ρ^{*II}	$\beta\mu_A^{*I}$	$\beta\mu_A^{*II}$	$\beta\Delta\mu_{BA}^{*I}$	$\beta\Delta\mu_{BA}^{*II}$	$\beta\Delta\mu_{AB}^{*I}$	$\beta\Delta\mu_{AB}^{*II}$
0.023	0.019 (8)	0.025 (1)	0.039 (1)	0.103 (1)	0.2511 (8)	0.0137 (8)	−6.68 (3)	−6.78 (1)	2.03 (1)	2.04 (1)	−1.97 (2)	−2.06 (1)
0.024	0.028 (1)	0.024 (1)	0.049 (1)	0.119 (1)	0.2509 (8)	0.0147 (3)	−6.40 (5)	−6.59 (1)	1.88 (1)	1.86 (1)	−1.66 (10)	−1.88 (1)
0.026	0.027 (9)	0.026 (1)	0.101 (2)	0.216 (3)	0.2581 (9)	0.0160 (1)	−5.72 (2)	−5.93 (3)	1.13 (3)	1.16 (3)	−1.24 (11)	−1.18 (1)
0.029	0.029 (9)	0.029 (2)	0.221 (2)	0.352 (1)	0.2604 (21)	0.0183 (2)	−5.10 (7)	−5.33 (2)	0.42 (2)	0.50 (1)	−0.27 (2)	−0.55 (3)
0.032	0.037 (13)	0.033 (1)	0.391 (15)	0.489 (17)	0.2800 (29)	0.0216 (11)	−4.22 (1)	−4.87 (2)	:0.11 (1)	−0.10 (5)	0.22 (27)	0.57 (9)
0.035	0.007 (26)	0.035 (1)	0.513 (5)	0.597 (1)	0.2936 (122)	0.0223 (4)	−3.84 (2)	−4.63 (1)	−0.42 (4)	−0.47 (2)	0.48 (27)	0.50 (4)
0.032	−0.029 (19)	0.034 (1)	0.773 (6)	0.740 (5)	0.3347 (60)	0.0213 (3)	−3.08 (17)	−4.43 (1)	−1.17 (13)	−1.12 (1)	1.53 (6)	1.10 (1)
0.031	−0.083 (65)	0.030 (1)	0.953 (3)	0.910 (2)	0.3839 (14)	0.0186 (1)	−2.42 (11)	−4.31 (1)	−2.36 (2)	−2.34 (3)	2.66 (19)	2.34 (3)
0.029	−0.394 (310)	0.028 (11)	0.955 (65)	0.914 (1)	0.3825 (39)	0.0174 93)	−2.46 (15)	−4.35 (1)	−2.40 (6)	−2.39 (4)	2.85 (7)	2.39 (2)

[a] The numbers in parentheses indicate the statistical uncertainties in the last digits. $P^* = \rho\sigma^3/\epsilon$; $\rho^* = \rho\sigma^3$; $\mu^* = \mu/\epsilon$.

TABLE 7: Simulation Results for the Ternary Mixture $CH_4 + CO_2 + C_2H_6$ at $T = 250.5$ K and $P = 30.4$ bar[a]

P^{*I}	P^{*II}	ρ^{*I}	ρ^{*II}	x_A^I	x_B^I	x_A^{II}	x_B^{II}	$\beta\mu_A^{*I}$	$\beta\mu_A^{*II}$	$\beta\Delta\mu_{BA}^{*I}$	$\beta\Delta\mu_{BA}^{*II}$	$\beta\Delta\mu_{CA}^{*I}$	$\beta\Delta\mu_{CA}^{*II}$
0.080 (8)	0.076 (2)	0.4700 (30)	0.0591 (7)	0.142 (3)	0.118 (4)	0.434 (5)	0.146 (3)	−3.97 (4)	−3.98 (1)	−1.08 (6)	−1.20 (4)	−0.28 (1)	−0.35 (1)
0.079 (9)	0.075 (1)	0.4823 (19)	0.0578 (1)	0.113 (2)	0.251 (6)	0.356 (1)	0.270 (5)	−4.14 (2)	−4.19 (1)	−0.34 (12)	−0.40 (2)	−0.25 (6)	−0.26 (1)
0.079 (3)	0.075 (1)	0.5261 (22)	0.0582 (6)	0.074 (3)	0.484 (4)	0.260 (4)	0.446 (4)	−4.43 (5)	−4.49 (2)	0.57 (8)	0..35 (5)	−0.20 (1)	−0.20 (2)
0.070 (17)	0.076 (1)	0.6010 (38)	0.0585 (7)	0.054 (1)	0.742 (7)	0.250 (4)	0.573 (9)	−4.48 (4)	−4.51 (1)	0.78 (5)	0.61 (1)	−0.70 (1)	−0.63 (2)
0.075 (3)	0.075 (1)	0.6393 (57)	0.0564 (1)	0.050 (1)	0.828 (1)	0.269 (2)	0.607 (2)	−4.38 (4)	−4.46 (1)	0.70 (4)	0.62 (1)	−1.04 (2)	−1.06 (1)

[a] The numbers in parentheses indicate the statistical uncertainties in the last digits. $P^* = p\sigma^3/\epsilon$; $\rho^* = \rho\sigma^3$; $\mu^* = \mu/\epsilon$.

C_2H_6. In the ternary mixture $CH_4-C_2H_6-CO_2$, transfer was applied to CH_4 and exchange to CH_4/C_2H_6 and CH_4/CO_2.

5. Results and Discussion

For the binary mixtures, the simulations were performed at $T = 250$ K and $P = 20-80$ bar for CH_4-CO_2, 15−65 bar for $CH_4-C_2H_6$, and 14−21.5 bar for $C_2H_6-CO_2$. For the ternary mixture $CH_4-C_2H_6-CO_2$ the simulations were performed at $P = 30.4$ bar. The results are presented in Tables 3−7 and plotted in Figures 1−4 together with literature data. The results are in good agreement with experimental data and data from other simulation techniques applying the same molecular models. In the test particle method, chemical potentials are evaluated in a "nondestructive" way and the phase equilibria are determined indirectly. In general, the uncertainties in pressure and density from our simulations have larger fluctuations than those from the test particle method. In those simulations, 500 particles were used, whereas about half of that number was located in each box in our simulations. The numbers in parentheses indicate the statistical uncertainties in the last digits.

The results for the binary mixtures $CH_4-C_2H_6$ in Table 4 are reduced by the parameters of CH_4. We calculated the pressures and chemical potentials in each box during the simulations. In Table 4 A stands for CH_4 and B for C_2H_6. The suffix BA means the difference between the component B and component A evaluated by exchanging a particle of A to a particle of B and vice versa for AB. From the data we can see

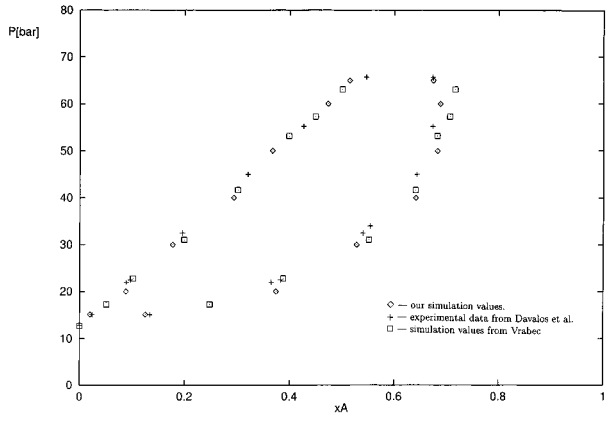

Figure 1. . Vapor−liquid equilibria of methane + ethane at $T = 250$ K: ◇, simulation values; +, experimental data from Davalos et al.;[16] □, simulation values from Vrabec.[15]

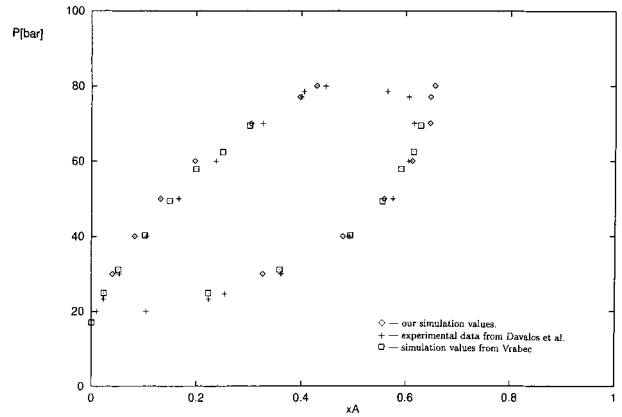

Figure 2. Vapor−liquid equilibria of methane + carbon dioxide at T = 250 K: ◇, simulation values; +, experimental data from Davalos et al.;[16] □, simulation values from Vrabec.[15]

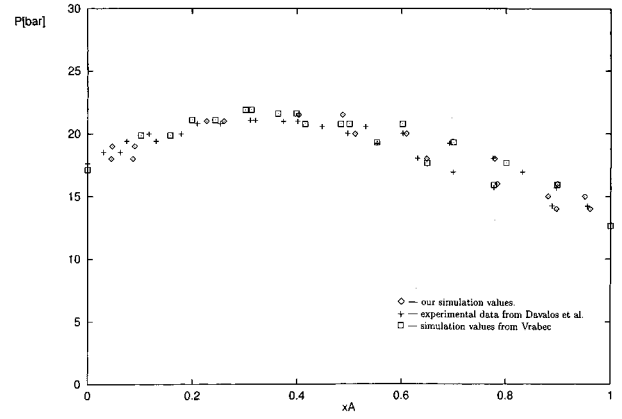

Figure 3. Vapor−liquid equilibria of ethane + carbon dioxide at T = 250 K: ◇, simulation values; +, experimental data from Davalos et al.;[16] □, simulation values from Vrabec.[15]

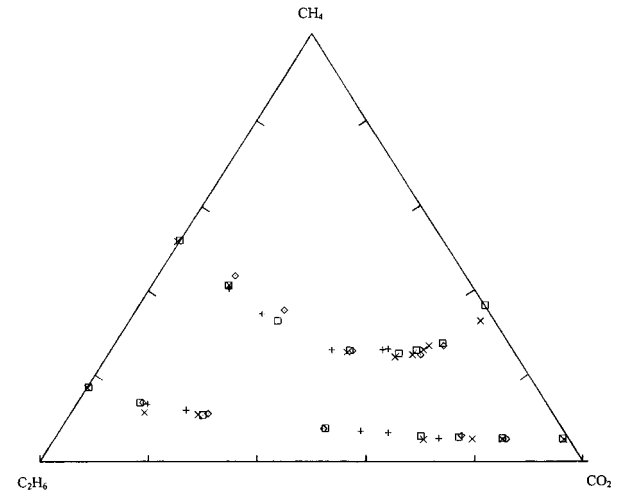

Figure 4. Vapor−liquid equilibria of methane + ethane + carbon dioxide at T = 250.5 K and P = 30.4 bar: ◇, simulation values; +, experimental data from Davalos et al.;[16] □, simulation values from Vrabec;[15] ×, experimental data from Knapp et al.[22]

that the equilibrium between the two phases is established through the approximate equalities of pressures, the chemical potentials of methane, and the chemical potential differences between methane and ethane in the two boxes. The pressure in the liquid phase has larger uncertainties than that in the vapor phase, which suggests that the fluctuation of particles has more influence on the liquid phase and the pressure is slowly adjusted to the imposed pressure. One interesting point to notice is that the chemical potential difference in the liquid phase (columns 10 and 12) can only be evaluated correctly by exchange of methane to ethane, whereas the chemical potential difference in the vapor phase (columns 11 and 13) can be approached from both directions of exchange. Figure 1 displays the $P-x$ data for methane + ethane in comparision with literature data. In general, our values are in very good agreement with the MD simulation data from Vrabec[15] and with the experimental data from Davalos et al.[16]

The results for the binary mixture CH_4-CO_2 in Table 5 are also reduced by the parameters of CH_4, and the $P-x$ data are presented in Figure 2 with literature data. The figure shows that our data are close to the data from Vrabec,[15] and both methods produced separation curves shifted slightly to the liquid side and extended to higher pressures compared with the experimental data. The large deviations from the experimental data occur above 70 bar. The deviation may be caused by the uncertainty of the cross-interaction parameters, which were determined by fitting excess quantities from EOS data.[15] Neverthless, both simulation techniques yielded satisfactory results.

The results for the binary mixture $CO_2 + C_2H_6$ are presented in Table 6. These mixtures are thermodynamically very interesting, because carbon dioxide and ethane have close critical temperatures ($T_c[CO_2]$ = 304.15 K; $T_c[C_2H_6]$ = 305.3 K) and the mixture possesses an azeotrope at T = 250.5 K. Carbon dioxide is modeled as a two-center LJ plus point quadrupole fluid and ethane as a two-center LJ fluid. Carbon dioxide can be regarded as a thinner object than ethane; exchange of carbon dioxide to ethane, therefore, produced better results. From the chemical potentials of carbon dioxide in Table 6 we can see that the chemical potentials in the liquid phase (column 8) deviate systematically from those in the vapor phase with an increase of the CO_2 concentration, which indicates that the insertion of particles becomes inefficient. Figure 3 displays the $P-x$ data for $CO_2 + C_2H_6$ in comparison with literature data. Except near the azeotrope region, the agreement with the literature data is good.

The simulation results for the ternary mixture $CH_4 + C_2H_6 + CO_2$ are presented in Table 7. At the simulated temperature and pressure, there were no problems for the trial moves of the three components. The liquid-phase−vapor-phase separations were determined in excellent agreement with experimental data and the data from the test particle method. The maximum deviation in concentration was estimated at less than 3% for low concentrations of CO_2. The composition phase equilibrium data of the ternary mixtures together with literature data are displayed in Figure 4. The results indicate first that the modified Gibbs ensemble method proposed by Panagiotopoulos and the procedure used in this work can be applied efficiently to determine phase equilibria of chemically realistic multicomponents as long as the effective interaction potentials are accurate. Second, the results also verify the conclusion from Vrabec and Fischer[9] that there is no need to introduce additional parameters for the ternary mixture of $CH_4 + C_2H_6 + CO_2$. In the literature, Gibbs ensemble techniques have been utilized to examine liquid−vapor equilibria of long-chain alkanes[6,7] and alkane mixtures,[8] and several simulations of mixtures have been performed on systems consisting of spherical LJ molecules.[3−5] The present work lends further evidence that more complicated molecular models for multicomponent mixtures can be realistically examined with Gibbs ensemble simulation. Since the *NpT* + test particle method applies an indirect and nondestructive

approach for determining the phase behavior of fluids, the results have smaller uncertainties for liquid−vapor equilibria in general. However, for determination of one binodal, four simulations are usually needed in the *NpT*−test particle method, whereas only one simulation is needed in the Gibbs method. The directness and time saving may be the most appealing advantages of the Gibbs method. In addition, the Gibbs method can be applied to simulate liquid-phase−liquid-phase equilibria as long as one component can be transferred between the simulation boxes.[17] In our ternary simulations, particle exchanges were between CH_4/C_2H_6 and CH_4/CO_2, with no exchanges between CO_2/C_2H_6. We could also apply particle exchanges to CH_4/CO_2 and CO_2/C_2H_6, through which the chemical equilibrium of C_2H_6, the largest molecule, can be established stepwise.

Thermodynamic derivatives can be obtained by switching particles,[18−20] which can be used to extrapolate phase separation curves to different temperatures and pressures.[21] An interesting question is whether the information obtained from the transfer/exchange of particles can also be utilized to extrapolate the phase separation curves in the Gibbs ensemble simulation. If the temperature and pressure dependences of the chemical potentials could be accurately calculated in the Gibbs ensemble, the number of simulations would be dramatically reduced in determination of phase equilibria over a wide range of conditions. We are now in the process of exploring such a possibility. Applications to hydrogen bonded fluids should also prove interesting (and challenging) since a mixture such as CO_2/CH_3OH is important for such separation processes as supercritical fluid chromatography.

Acknowledgment. The authors thank the National Science Foundation (Grant CHE-9632309) for support of this research and the Ohio Supercomputer Center for providing the computer time. We also thank Dr. Daan Frenkel for interesting discussions and for support during a sabbatical leave (T.L.B.) at the FOM Institute in Amsterdam.

References and Notes

(1) Panagiotopoulos, A. Z. *Mol. Phys.* **1987**, *61*, 813.
(2) Gubbins, K. *Fluid Phase Equilib.* **1993**, *83*, 1.
(3) Panagiotopoulos, A. In *Supercritical Fluid Science and Technology*; Johnston, K. P., Penninger, J. M. L., Eds.; ACS Symposium Series, Vol. 406; American Chemical Society, New York, 1989; p 39.
(4) Green, D. G.; Jackson, G.; Miguel, E.; Rull, L. F. *J. Chem. Phys.* **1994**, *101*, 3190.
(5) Harismiadus, V. I.; Koutras, N. K.; Tassios, D. P. *Fluid Phase Equilib.* **1991**, *65*, 1.
(6) Siepmann, J. I.; Karaborni, S.; Smit, B. *Nature* **1993**, *365*, 330.
(7) Mooij, G. C. A. M.; Frenkel, D.; Smit, B. *J. Phys. Condens. Matter* **1992**, *4*, L255.
(8) Martin, M. G.; Siepmann, J. I. *J. Am. Chem. Soc.* **1997**, *119*, 8921.
(9) Vrabec, J.; Fischer, J. *Int. J. Thermophys.* **1996**, *17*, 889.
(10) Liu, A. *Mol. Simul.* **1996**, *17*, 75.
(11) Panagiotopoulos, A. Z. *Int. J. Thermophys.* **1989**, *10*, 447.
(12) Lotfi, A. Ph.D. thesis at Ruhr-University Bochum, Germany 1993.
(13) Möller, D.; Óprzynski, J.; Müller, J.; Fischer, J. *Mol. Phys.* **1992**, *75*, 363.
(14) Smit, B.; Frenkel, D. *Mol. Phys.* **1989**, *68*, 951.
(15) Vrabec, J. Ph.D. thesis at Ruhr-University Bochum, Germany, 1996.
(16) Davalos, J.; Anderson, W.; Phelps, R.; Kidnay, A. *J. Chem. Eng. Data* **1976**, *21*, 81.
(17) de Kuijper, A.; Smit, B.; Schouten, J. A.; Michels, J. P. J. *Europhys. Lett.* **1990**, *13*, 679.
(18) Sindzingre, P.; Ciccotti, G.; Massobrio, C.; Frenkel, D. *Chem. Phys. Lett.* **1987**, *136*, 35.
(19) Sindzingre, P.; Massobrio, C.; Ciccotti, G.; Frenkel, D. *Chem. Phys.* **1989**, *129*, 213.
(20) Shing, K. *Chem. Phys. Lett.* **1985**, *119*, 149.
(21) Liu, A.; Beck, T. L. *J. Chem. Phys.* **1996**, *105*, 2424.
(22) Knapp, H.; Yang, X.; Zhang, Z. *Fluid Phase Equilib.* **1990**, *54*, 1.